p53 Regulates Mitochondrial Respiration

Satoaki Matoba *et al.*

Science **312**, 1650 (2006);
DOI: 10.1126/science.1126863

reproduces the observed distribution coefficients in both P-rich and P-poor experiments. This behavior implies that phosphorous, at least at geologically relevant concentration levels, does not influence partition coefficients through complexing with trace cations, as proposed by (*28*), but rather influences partitioning indirectly by affecting NBO/BO ratios. Specifically, elements such as P with high coordination numbers lower the melt NBO/BO ratio and decrease the configurational entropy of the melt, an effect that widens the MO_n-C_oO_p solvus and increases melt-melt partition coefficients. Within the di- and trivalent cations, such a tendency is observable in our data; i.e., partition coefficients decrease with decreasing coordination number.

Our data imply that a significant change in the shape of the lattice-strain model parabola will result for the alkalis. To quantify this effect, we used data sets of $D^{cpx/basalt}$ (*30*, *31*) for basalts analogous to the gabbroic melt of experiment Z10 and combine $D^{cpx/basalt}$ with our $D^{basalt/granite}$. The site parameters for monovalent cations calculated from $D^{cpx/granite}$ with respect to $D^{cpx/basalt}$ are characterized by a Young's modulus decreased by 16 to 35% and by a strain-free partition coefficient D_0 increased by a factor of 2. This softening of the site is attributed to the effect of melt composition. For the cations coordinated to NBOs, the effect of melt composition will increase $D^{crystal/melt}$, D_o, and hence the position of the parabola with respect to the D coordinate (*1*, *5*) by one order of magnitude when changing from basaltic to granitic melt compositions. This effect acts in concert with the changes in crystal composition that occur as a consequence of the change in melt composition. Melt composition will play a key role for elements whose crystal/melt partition coefficients are close to unity, because they may change from compatible to incompatible as a function of melt composition. Because of the relative uniformity of partition coefficients for traces of Ca, Mg, RE, transition, and high field strength elements, melt composition does not strongly affect the relative partition coefficients of these elements. The latter are in general well characterized by models describing relative crystal-melt partition coefficients solely in terms of crystal lattice strain, but to quantify individual partition coefficients an explicit melt compositional term such as in Eq. 4 is necessary. Gross exceptions to the above generality are Pb (Fig. 2), for which $D^{gabbro/granite}$ is as much as two orders of magnitude different from other divalent cations, and to a lesser extent Ba, Zn, and Sn. Among the NBO-coordinated cations, variations of $D^{basalt/granite}$ up to a factor of 2 exist, a nonnegligible effect in the context of geochemical melting models.

References and Notes

1. N. Onuma, H. Higuchi, H. Wakita, H. Nagasawa, *Earth Planet. Sci. Lett.* **5**, 47 (1968).
2. J. C. Brice, *J. Cryst. Growth* **28**, 249 (1975).
3. S. Banno, Y. Matsui, *Chem. Geol.* **11**, 1 (1973).
4. M. J. Drake, D. F. Weill, *Geochim. Cosmochim. Acta* **39**, 689 (1975).
5. J. D. Blundy, B. J. Wood, *Nature* **372**, 452 (1994).
6. B. J. Wood, J. D. Blundy, *Geochim. Cosmochim. Acta* **66**, 3647 (2002).
7. B. J. Wood, J. D. Blundy, *Contrib. Mineral. Petrol.* **129**, 166 (1997).
8. E. B. Watson, *Contrib. Mineral. Petrol.* **56**, 119 (1976).
9. F. J. Ryerson, P. C. Hess, *Geochim. Cosmochim. Acta* **42**, 921 (1978).
10. B. O. Mysen, D. Virgo, *Geochim. Cosmochim. Acta* **44**, 1917 (1980).
11. R. L. Linnen, H. Keppler, *Geochim. Cosmochim. Acta* **66**, 3293 (2002).
12. B. O. Mysen, E. V. Dubinsky, *Geochim. Cosmochim. Acta* **68**, 1617 (2004).
13. M. W. Schmidt, A. Dardon, G. Chazot, R. Vannucci, *Earth Planet. Sci. Lett.* **226**, 415 (2004).
14. S. Klemme, S. Prowatke, K. Hametner, D. Günther, *Geochim. Cosmochim. Acta* **69**, 2361 (2005).
15. I. V. Veksler, C. Petibon, G. A. Jenner, A. M. Dorfman, D. B. Dingwell, *J. Petrol.* **39**, 2095 (1998).
16. E. Roedder, *Geochim. Cosmochim. Acta* **42**, 1597 (1978).
17. W. Visser, A. F. K. VanGroos, *Am. J. Sci.* **279**, 70 (1979).
18. Material and methods are available as supporting material on *Science* Online.
19. Previous studies (*8*, *9*) have shown that 14 hours are sufficient to reach chemical equilibrium in this temperature range; we thus generally doubled this run time.
20. R. L. Lange, I. S. E. Carmicheal, *Rev. Mineral.* **24**, 25 (1990).
21. At 1180°C, the two melts have SiO_2 contents of 72.2 and 37.1 weight %; at 1210°C, the immiscibility gap is closed, which is in excellent agreement with (*16*, *17*).
22. Electronegativities are from (*32*).
23. R. D. Shannon, *Acta Cryst.* **A32**, 751 (1976).
24. Ionic radii are those for the dominant coordination number as listed in table S1.
25. L. Galoisy *et al.*, *Mineral. Mag.* **64**, 409 (2000).
26. F. J. Ryerson, P. C. Hess, *Geochim. Cosmochim. Acta* **44**, 611 (1980).
27. B. O. Mysen, *Structures and Properties of Silicate Melts,* vol. 4 of *Developments in Geochemistry* (Elsevier, Amsterdam, 1988).
28. A. J. G. Ellison, P. C. Hess, *Geochim. Cosmochim. Acta* **53**, 1965 (1989).
29. W. Visser, A. F. K. VanGroos, *Am. J. Sci.* **279**, 970 (1979).
30. J. D. Blundy, J. Dalton, *Contrib. Mineral. Petrol.* **139**, 356 (2000).
31. R. A. Brooker *et al.*, *Nature* **423**, 738 (2003).
32. R. D. Lide, Ed., *The Handbook of Chemistry and Physics* (CRC Press, Boca Raton, FL, ed. 85, 2005), table 9-74.
33. W. R. H. Ramsey, A. J. Crawford, J. D. Fodon, *Contrib. Mineral. Petrol.* **88**, 386 (1984).
34. H. Sorenson, Ed., *The Alkaline Rocks* (Wiley, Letchworth, UK, 1974), p. 117.

35. We thank N. Baker from *g-max* for building the centrifuge and K. Hametner for help with the LA-ICP-MS analyses. M.W.S. acknowledges Swiss National Science Foundation grant no. 2-77182-02 for financing part of the centrifuge.

Supporting Online Material

www.sciencemag.org/cgi/content/full/312/5780/1646/DC1
Materials and Methods
SOM Text
Table S1
References

24 February 2006; accepted 25 April 2006
10.1126/science.1126690

p53 Regulates Mitochondrial Respiration

Satoaki Matoba,[1] Ju-Gyeong Kang,[1] Willmar D. Patino,[1] Andrew Wragg,[1] Manfred Boehm,[1] Oksana Gavrilova,[2] Paula J. Hurley,[3] Fred Bunz,[3] Paul M. Hwang[1]*

The energy that sustains cancer cells is derived preferentially from glycolysis. This metabolic change, the Warburg effect, was one of the first alterations in cancer cells recognized as conferring a survival advantage. Here, we show that p53, one of the most frequently mutated genes in cancers, modulates the balance between the utilization of respiratory and glycolytic pathways. We identify Synthesis of Cytochrome c Oxidase 2 (SCO2) as the downstream mediator of this effect in mice and human cancer cell lines. SCO2 is critical for regulating the cytochrome c oxidase (COX) complex, the major site of oxygen utilization in the eukaryotic cell. Disruption of the *SCO2* gene in human cancer cells with wild-type p53 recapitulated the metabolic switch toward glycolysis that is exhibited by p53-deficient cells. That SCO2 couples p53 to mitochondrial respiration provides a possible explanation for the Warburg effect and offers new clues as to how p53 might affect aging and metabolism.

Cancer is a genetic disease caused by the dysregulation of various cellular pathways that orchestrate cell growth and death (*1*). It is clear that some of these pathways must modulate cellular metabolism. As described by Otto Warburg in 1931, cancer cells preferentially utilize glycolytic pathways for energy generation while down-regulating their aerobic respiratory activity (*2*). A number of mechanisms have been proposed to explain the Warburg effect (*3*–*7*), but there have not been any reports of a genetically defined pathway that couples a tumor suppressor gene to mitochondrial aerobic respiration.

Critical to aerobic life is the cytochrome c oxidase (COX) complex in the mitochondrion, where most of the molecular oxygen is consumed in the eukaryotic cell. In cancer cells mitochondrial respiratory activity is decreased in association with changes in the expression levels of COX complex subunit proteins, but the genetic mechanisms that underlie their modulation are unclear (*8*, *9*). We reasoned that because the metabolic alterations of cancer cells are

so widespread, an explanation for this phenomenon must lie, at least in part, in a pathway that is commonly altered in cancer cells. We therefore examined whether alteration of p53, the gene most commonly mutated in human cancer, might affect COX complex assembly and activity.

Aerobic respiration was assessed in liver mitochondria preparations from mice with wild-type (+/+), heterozygous (+/−), or homozygous (−/−) disruption of *TP53*. There was a significant decrease in oxygen consumption that closely correlated with p53 deficiency ($p53^{+/+}$ versus $p53^{-/-}$, $P < 0.001$) (Fig. 1A). We confirmed a similar p53-dependent reduction (~25%) in cellular oxygen consumption using isogenic human colon cancer HCT116 cells with a targeted disruption of *TP53* (Fig. 1A) (*10*). Direct measurement of COX enzymatic activity showed a comparable reduction of 25 ± 3% in the $p53^{-/-}$ cells (fig. S1). To estimate the relative contributions of glycolysis and aerobic respiration, we calculated total adenosine 5′-triphosphate (ATP) generated by measuring whole-cell lactate production and oxygen consumption, respectively (*11*). The total amount of ATP measured was similar in all three genotypes, but the p53-deficient cells produced significantly higher levels of lactate, indicating a change in the mode of energy production to one favoring glycolysis (Fig. 1B). The ratio of ATP produced by glycolysis versus ATP produced by aerobic respiration increased with p53 deficiency: $p53^{+/+}$, 0.81 ± 0.12; $p53^{+/-}$, 1.04 ± 0.20; and $p53^{-/-}$, 1.72 ± 0.16 (Fig. 1B).

Our results indicated that $p53^{-/-}$ mice exhibit decreased mitochondrial respiration, which could translate into a decrease in functional aerobic capacity. The general appearance and behavior of $p53^{+/+}$ and $p53^{-/-}$ mice were indistinguishable, as previously observed (*12*), and their body mass and composition were essentially identical (Fig. 1C). However, the endurance of $p53^{-/-}$ mice was reduced, as measured by a swimming stress test (Fig. 1D) (*13*).

Because p53 is a transcriptional activator, we reasoned that a gene regulated by p53 might mediate this effect on mitochondrial respiration. We examined a serial analysis of gene expression (SAGE) database of potential p53 target genes (*14*) that may influence mitochondrial function. SCO2 (Synthesis of Cytochrome c Oxidase 2) was induced in a p53-dependent manner in HCT116 cells, as evidenced by a ninefold increase in transcripts. On the basis of more recent genetic and biochemical studies (*15*, *16*), we reasoned that SCO2 could potentially mediate the effect of p53 on aerobic respiration. SCO2 is required for the assembly of mitochondrial DNA-encoded COX II subunit (*MTCO2* gene) into the COX complex, and inactivating mutations of this gene in humans result in fatal cardioencephalomyopathy due to aerobic respiratory failure (*17*).

To confirm that SCO2 transcription is directly transactivated by p53, we used human colon cancer DLD1 cell lines with either inducible wild-type (WT) or mutant (MUT) p53 for expression studies (*18*). SCO2 mRNA expression increased within 3 to 18 hours of induced WT p53 expression but was not affected by mutant p53 (Fig. 2A and fig. S2). We also measured the mRNA expression level of SCO1, another COX assembly factor. SCO1 mRNA expression remained unchanged with induced p53 expression, serving as a negative control and demonstrating the specificity of the observed SCO2 mRNA increase (Fig. 2A).

The time course of SCO2 transcription and the presence of p53 DNA-binding consensus sequence in intron 1 (−322 to –302 from the start codon) suggested that SCO2 may be directly transactivated by p53. We tested this hypothesis by cloning a ~1.1-kb fragment of the SCO2 gene containing the p53-binding sequence into a luciferase reporter plasmid. To control for the nonspecific effects of endogenous p53, we used the $p53^{-/-}$ HCT116 cell line to express the reporter and exogenous p53 plasmids. As predicted for a specific p53 binding site, we observed increases in luciferase activity that were dependent on the dose of exogenous WT p53 (pCMV-p53) but not mutant p53 (pCMV-p53mt135) (Fig. 2B). When the p53 binding sequence in the reporter construct was mutated, the transcriptional activation by exogenous WT p53 was abrogated, establishing its in vitro specificity (Fig. 2B).

Antibodies against SCO2 were generated and used to determine the expression of SCO2. SCO2 protein expression decreased in both p53-deficient mouse liver mitochondria and human cell lines, whereas the amount of mitochondrial anion transporter (voltage-dependent anion channel, or VDAC) remained constant (Fig. 2C). Although p53 transactivates SCO2, the amounts of SCO2 protein detected in the $p53^{-/-}$ mice and human cells indicate that p53-independent pathways exist for its regulation, as is the case for other p53-target genes (Fig. 2C) (*19*). In contrast to SCO2 expression, the level of SCO1 protein was unaffected by p53 genotype status, consistent with transcriptional data (Fig. 2C and fig. S2). These results suggested a direct interaction between p53 and SCO2 to regulate mitochondrial aerobic respiration.

Expression of WT SCO2 cDNA in $p53^{-/-}$ HCT116 cells increased mitochondrial oxygen consumption within 48 hours in a dose-dependent manner (Fig. 3A). The amount of SCO2 protein needed to rescue the deficit in mitochondrial respiration of the $p53^{-/-}$ cells corresponded well to the physiological levels observed in the $p53^{+/+}$ cells (Fig. 3A). Oxygen consumption also increased with SCO2 expression in human colon cancer cell lines with naturally occurring p53 mutations (DLD1 and

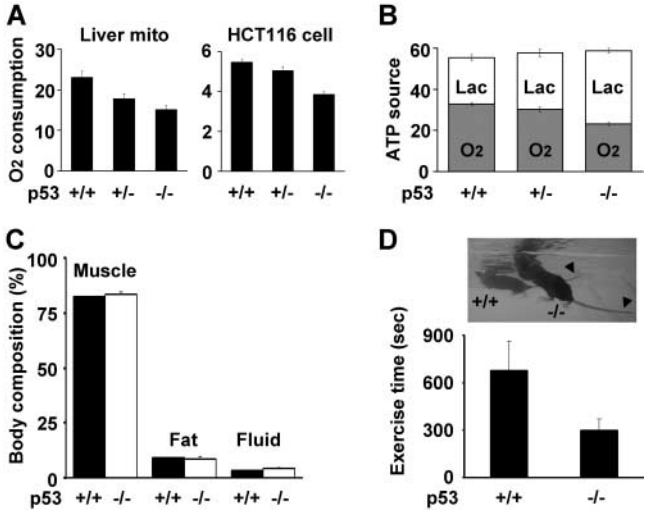

Fig. 1. Dependence of aerobic respiration, glycolysis, and exercise capacity on p53. (**A**) Oxygen consumption (mean ± SD, nmol min^{-1} mg^{-1} protein) was measured by a Clark-type oxygen microelectrode in mouse liver mitochondria preparations and in HCT116 cells with three *TP53* genotypes: wild-type (+/+), heterozygous (+/−), and homozygous disruption (−/−). (**B**) The amount of ATP (mean ± SD, nmol min^{-1} mg^{-1} protein) produced by aerobic respiration (gray bars, O_2) and glycolysis (light bars, Lac) was calculated by measuring oxygen consumption and lactate production in the three different *TP53* genotypes of HCT116 cells. (**C**) Body mass composition of muscle, fat, and free fluid (percentage of total) was determined in nonanesthetized age- and sex-matched mice using a nuclear magnetic resonance analyzer. Body mass (mean ± SD) for the $p53^{+/+}$ and $p53^{-/-}$ mice was 20.4 ± 1.2 g and 20.1 ± 1.9 g, respectively. p53 genotypes indicated for wild-type (+/+) (dark bars, $n = 5$) and homozygous knockout (−/−) (light bars, $n = 5$) mice. (**D**) Maximum duration of swimming exercise measured in a temperature-controlled adjustable-current tank. Exercise time (mean ± SD, s) to the point of exhaustion, as indicated by inability to stay afloat, is shown for each genotype ($P = 0.008$, $n = 5$ for each group). Note that the $p53^{-/-}$ mouse (foreground) assumes a more vertical posture consistent with early fatigue, in contrast to the wild-type mouse (background) with horizontal body and tail positions (arrowheads) (*13*).

[1]Cardiology Branch, National Heart, Lung, and Blood Institute, [2]Diabetes Branch, National Institute of Diabetes and Digestive and Kidney Diseases, National Institutes of Health, Bethesda, MD 20892, USA. [3]Department of Radiation Oncology and Molecular Radiation Sciences, The Sidney Kimmel Comprehensive Cancer Center, The Johns Hopkins School of Medicine, Baltimore, MD 21231, USA.

*To whom correspondence should be addressed. E-mail: hwangp@mail.nih.gov

SW480 cells), suggesting that SCO2 expression can generally rescue oxygen consumption in p53-deficient cells (Fig. 3A).

To rule out the possibility that decreased mitochondrial respiration in the $p53^{-/-}$ HCT116 cells may result from chronic metabolic or other unrelated genetic changes that may have occurred during clonal selection, we examined oxygen consumption after reducing p53 expression by small interfering RNA (siRNA). Decreased p53 expression in parental HCT116 cells resulted in decreased SCO2 protein expression and reduced oxygen consumption within 48 hours, phenocopying the p53-deficient cells (Fig. 3B).

To genetically test whether p53 regulates mitochondrial respiration through SCO2, we disrupted the *SCO2* locus by homologous recombination in the human HCT116 cell line. Elimination of one of the two *SCO2* alleles could phenocopy the p53-deficient cells through the direct reduction of SCO2 expression. A targeting vector was designed to remove about 500 base pairs of SCO2 coding sequence upon homologous recombination into the *SCO2* locus. This construct was assembled into a recombinant adeno-associated virus (rAAV) (*20*). After viral transduction and screening of 1200 drug-selected clones, we identified three independently derived clones that gave the appropriately sized knockout (KO) polymerase chain reaction (PCR) product, indicating successful disruption of the *SCO2* allele (Fig. 4A). The amounts of SCO2 protein in each of the three $SCO2^{+/-}$ (H1 to H3) knockout clones were reduced relative to that in the WT parental (P) and sister clones (S1 and S2) that had also undergone parallel viral transduction and selection processes (Fig. 4A). Cell viability and growth rates were similar for the WT and $SCO2^{+/-}$ clones. However, the $SCO2^{+/-}$ cells displayed decreased oxygen consumption (O_2) and increased glycolytic activity (Lac) compared to WT cells, whereas total ATP concentrations remained the same, similar to the results for p53-deficient cells (Fig. 4B).

The direct regulation of aerobic respiration by p53 has important implications for understanding tumorigenesis. To date, much of the research on cellular processes driven by oncogenes and tumor suppressor genes has focused on the regulation of cell birth and death (*1*). Our study identifies a direct transcriptional target of p53 that modulates aerobic respiration and, by its haploinsufficiency, recapitulates the Warburg effect. It also defines a genetic pathway, not involving cell cycle regulation, by which the inactivation of p53 may promote tumorigenesis by decreasing cellular dependence on oxygen, potentially permitting growth in

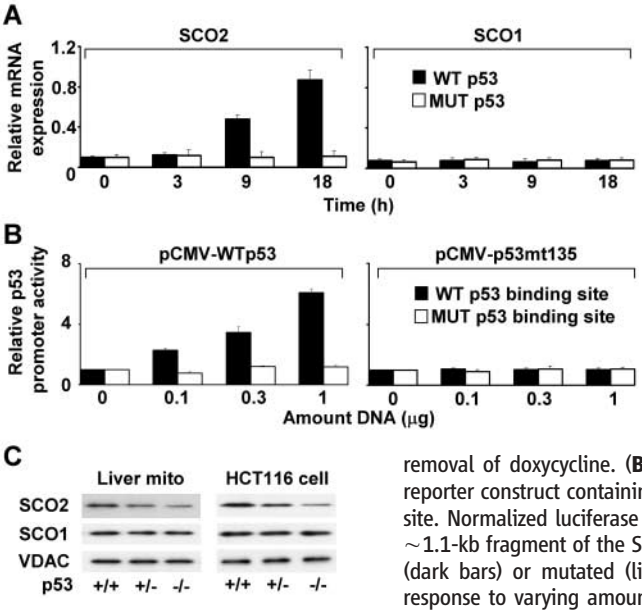

Fig. 2. Dependence of SCO2 mRNA transactivation and protein levels on p53. (**A**) SCO2 and SCO1 transactivation by wild-type (WT, dark bar) or mutant (MUT, light bar) p53 were measured using a modified tetracycline-inducible system in human colon cancer DLD1 cell line. mRNAs were quantified by real-time reverse transcription (RT)–PCR and normalized to a control gene *EIF3S5* (mean ± SD, relative value). Time (in hours) indicates induction by removal of doxycycline. (**B**) p53 transactivates luciferase reporter construct containing the *SCO2* gene p53 binding site. Normalized luciferase activity under the control of a ~1.1-kb fragment of the SCO2 gene containing wild-type (dark bars) or mutated (light bars) p53 binding site in response to varying amounts of wild-type (pCMV-p53) or mutant (pCMV-p53mt135) p53 transfection. (**C**) Dependence of SCO2 protein expression levels on p53 gene dosage in mouse liver mitochondria and HCT116 cells. Western blot analyses were done with specific antibodies against SCO2, SCO1, and VDAC proteins in mouse liver mitochondria and human HCT116 cell lines.

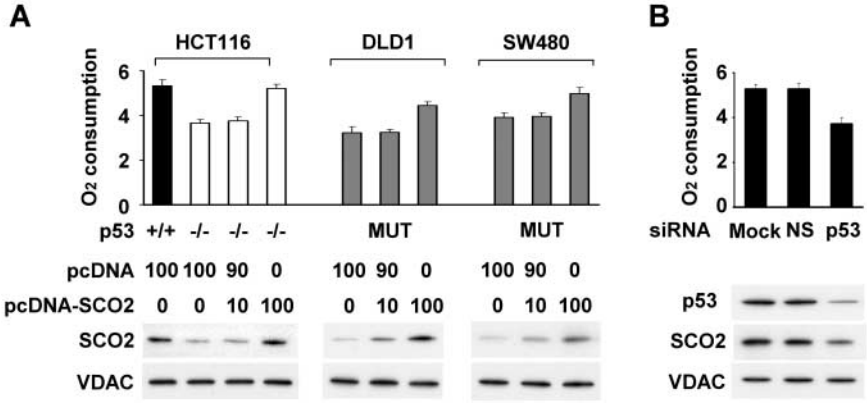

Fig. 3. Expression of SCO2 rescues alterations in mitochondrial respiration. (**A**) Transient transfection of SCO2 (pcDNA-SCO2, ng of DNA) into $p53^{-/-}$ HCT116 cells (light bars) increased SCO2 protein expression and oxygen consumption (mean ± SD, nmol min^{-1} mg^{-1} protein) to $p53^{+/+}$ (dark bar) levels. Control empty vector (pcDNA, ng of DNA) had no effect. Oxygen consumption was increased to wild-type HCT116 levels by SCO2 in p53-mutant (MUT) cell lines DLD1 and SW480 (gray bars). (**B**) Transient knockdown of p53 in wild-type HCT116 cells by sequence-specific siRNA (p53) decreases SCO2 protein and oxygen consumption (mean ± SD, nmol min^{-1} mg^{-1} protein). Mock (no siRNA) and nonspecific (NS) siRNA transfections had no effect.

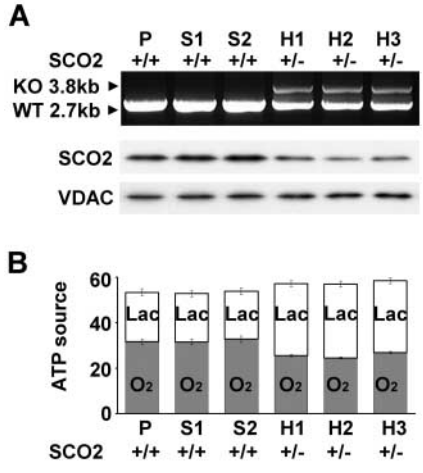

Fig. 4. Targeted disruption of one *SCO2* allele reproduces the p53-deficient metabolic phenotype. (**A**) Three clones (H1 to H3) with heterozygous disruption of *SCO2* were identified by the appearance of the 3.8-kb KO band accompanied by a decrease in the intensity of the 2.7-kb WT band. P is the parental cell line, and S1 and S2 are two sibling clones without SCO2 disruption. SCO2 protein expression levels were assessed by Western blotting. (**B**) The amount of ATP (mean ± SD, nmol min^{-1} mg^{-1} protein) produced by aerobic respiration (gray bars, O_2) and glycolysis (light bars, Lac) was calculated by measuring oxygen consumption and lactate production in the three wild-type (+/+) and three *SCO2* heterozygous (+/−) knockout clones.

more hypoxic environments. Two recent studies have implicated p53 in the control of glycolysis by its negative regulation of phosphoglycerate mutase (PGM) and Akt (*6*, *7*, *21*). Interestingly, despite the marked increase in glycolysis stimulated by Akt expression, cellular oxygen consumption remained stable, reflecting the tight homeostatic controls governing mitochondrial respiration (*22*). Additional functions of the *TP53* gene continue to be uncovered (*23*), and the effect of p53 status on exercise tolerance suggests that it has global functions that extend beyond processes related to cell birth and death (*24*). The COX complex is critical for aerobic eukaryotes, and *SCO2* and *MTCO2* (COX II) are ancient genes conserved in organisms as diverse as yeast and humans. The regulation of mitochondrial genome-encoded COX II by p53 suggests that our observations pertain to a fundamental control point in metabolism. Recent studies have implicated p53 as a mediator of senescence and aging (*25*–*27*), although specific aspects of this model remain controversial (*28*, *29*). Given the mounting evidence supporting a role for metabolism and oxidative stress in aging (*30*, *31*), the functional relationship between p53 and the COX complex assembly may underlie some aspects of organismal aging. In filamentous fungus, the genetic disruption of COX II markedly increases life-span (*32*). Future studies examining the role of p53 in mitochondrial regulation may clarify how a tumor suppressor gene can have such diverse and global effects on cellular and organismal functions.

References and Notes

1. B. Vogelstein, K. W. Kinzler, *Nat. Med.* **10**, 789 (2004).
2. O. Warburg, *Science* **124**, 269 (1956).
3. G. L. Semenza *et al.*, *Novartis Found. Symp.* **240**, 251 (2001).
4. N. C. Denko *et al.*, *Oncogene* **22**, 5907 (2003).
5. J. W. Kim *et al.*, *Mol. Cell. Biol.* **24**, 5923 (2004).
6. H. Kondoh *et al.*, *Cancer Res.* **65**, 177 (2005).
7. D. R. Plas, C. B. Thompson, *Oncogene* **24**, 7435 (2005).
8. P. C. Herrmann *et al.*, *Proteomics* **3**, 1801 (2003).
9. S. Zhou, S. Kachhap, K. K. Singh, *Mutagenesis* **18**, 287 (2003).
10. F. Bunz *et al.*, *Science* **282**, 1497 (1998).
11. S. Sariban-Sohraby, I. T. Magrath, R. S. Balaban, *Cancer Res.* **43**, 4662 (1983).
12. L. D. Attardi, L. A. Donehower, *Mutat. Res.* **576**, 4 (2005).
13. K. Matsumoto, K. Ishihara, K. Tanaka, K. Inoue, T. Fushiki, *J. Appl. Physiol.* **81**, 1843 (1996).
14. P. M. Hwang *et al.*, *Nat. Med.* **7**, 1111 (2001).
15. E. A. Shoubridge, *Am. J. Med. Genet.* **106**, 46 (2001).
16. P. Pecina, H. Houstkova, H. Hansikova, J. Zeman, J. Houstek, *Physiol. Res.* **53** (Suppl. 1), S213 (2004).
17. L. C. Papadopoulou *et al.*, *Nat. Genet.* **23**, 333 (1999).
18. J. Yu *et al.*, *Proc. Natl. Acad. Sci. U.S.A.* **96**, 14517 (1999).
19. B. Vogelstein, D. Lane, A. J. Levine, *Nature* **408**, 307 (2000).
20. M. Kohli, C. Rago, C. Lengauer, K. W. Kinzler, B. Vogelstein, *Nucleic Acids Res.* **32**, e3 (2004).
21. A. J. Levine, Z. Feng, T. W. Mak, H. You, S. Jin, *Genes Dev.* **20**, 267 (2006).
22. R. L. Elstrom *et al.*, *Cancer Res.* **64**, 3892 (2004).
23. L. J. Hofseth, S. P. Hussain, C. C. Harris, *Trends Pharmacol. Sci.* **25**, 177 (2004).
24. U. Wisloff *et al.*, *Science* **307**, 418 (2005).
25. S. D. Tyner *et al.*, *Nature* **415**, 45 (2002).
26. B. Maier *et al.*, *Genes Dev.* **18**, 306 (2004).
27. J. Campisi, *Cell* **120**, 513 (2005).
28. I. Garcia-Cao *et al.*, *EMBO J.* **21**, 6225 (2002).
29. M. V. Poyurovsky, C. Prives, *Genes Dev.* **20**, 125 (2006).
30. L. Bordone, L. Guarente, *Nat. Rev. Mol. Cell Biol.* **6**, 298 (2005).
31. R. S. Balaban, S. Nemoto, T. Finkel, *Cell* **120**, 483 (2005).
32. S. W. Stumpferl, O. Stephan, H. D. Osiewacz, *Eukaryot. Cell* **3**, 200 (2004).

33. We thank S. Nemoto, C. Mcleod, I. Pagel, C. Rago, and O. Mian for technical advice and assistance, and T. Finkel, M. N. Sack, N. Epstein, R. S. Balaban, and B. Vogelstein for helpful suggestions and critical reading of this manuscript. The p53-disrupted HCT116 cell lines, tetracycline-inducible p53 DLD1 cell lines, and plasmid constructs were gifts from B. Vogelstein and B. H. Park. This research was supported by the Division of Intramural Research, National Heart, Lung, and Blood Institute, NIH.

Supporting Online Material

www.sciencemag.org/cgi/content/full/1126863/DC1
Materials and Methods
Figs. S1 and S2
References and Notes

1 March 2006; accepted 17 May 2006
Published online 25 May 2006;
10.1126/science.1126863
Include this information when citing this paper.

The *Xist* RNA Gene Evolved in Eutherians by Pseudogenization of a Protein-Coding Gene

Laurent Duret,[1]* Corinne Chureau,[2] Sylvie Samain,[3] Jean Weissenbach,[3] Philip Avner[2]

The *Xist* noncoding RNA is the key initiator of the process of X chromosome inactivation in eutherian mammals, but its precise function and origin remain unknown. Although *Xist* is well conserved among eutherians, until now, no homolog has been identified in other mammals. We show here that *Xist* evolved, at least partly, from a protein-coding gene and that the loss of protein-coding function of the proto-*Xist* coincides with the four flanking protein genes becoming pseudogenes. This event occurred after the divergence between eutherians and marsupials, which suggests that mechanisms of dosage compensation have evolved independently in both lineages.

Mammalian X and Y chromosomes evolved from a pair of autosomes shortly after the divergence of mammals from other amniotes (*1*). In eutherians and in marsupials, the desiquilibrium in gene dosage between XY males and XX females is compensated for by silencing one of the X chromosomes in females (*2*–*4*). In eutherians, this silencing involves the *Xist* gene, which is located in the X inactivation center (*Xic*) and encodes a long untranslated RNA (*5*). *Xic* is located on the long arm of the human X chromosome, which corresponded to the proto–X chromosome in the mammalian cenancestor (last common ancestor) (*6*, *7*). This observation is consistent with the hypothesis that X-chromosome inactivation might have emerged contemporaneously with the chromosomal sex-determining mechanism, early in mammalian evolution (*8*).

To study the evolution of X inactivation, we searched for homologs of *Xist* in 14 vertebrate genomes (*9*). We found *Xist* in all eutherians (Fig. 1), which demonstrates that *Xist* was already present in the eutherian cenancestor. With BLAST, we failed to detect significant sequence similarity to *Xist* in noneutherian vertebrates.

In humans, the genomic region surrounding the *Xist* gene contains three protein-coding genes (*Cdx4*, *Chic1*, and *Xpct*) that have orthologs in all vertebrate classes (table S1). The linkage between these genes is conserved in chicken and in *Xenopus* (Fig. 2A). We will hereater refer to the genomic interval between *Chic1* and *Xpct* in noneutherian species as the *XicHR* (*Xic* homologous region). In eutherians, besides *Xist*, the *Xic* region contains two RNA genes (*Jpx* and *Ftx*) and two protein-coding genes (*Tsx* and *Cnbp2*) (*10*) (Fig. 2A). *Cnbp2* is a retrotransposed gene that is specific to eutherians (*9*). We failed to detect any homolog of *Tsx*, *Jpx*, or *Ftx* genes in noneutherian vertebrates. In both chicken and *Xenopus*, the *XicHR* contains five protein genes (*Fip1l2*, *Lnx3*, *Rasl11c*, *UspL*, and *Wave4)* that have no detectable orthologs in eutherian genomes (table S1). The gene content, order, and orientation of the *XicHR* is perfectly conserved between chicken and *Xenopus* (Fig. 2A), which indicates that the chicken *XicHR* (on an autosome) corresponds to the ancestral state in the tetrapod cenancestor.

To search for possible vestiges of *XicHR* genes in eutherians, we compared the chicken genomic sequence to its counterpart from four species representative of different eutherian orders

[1]Laboratoire de Biométrie et Biologie Evolutive (UMR 5558), CNRS and Université Lyon 1, 16 rue Raphaël Dubois, 69622 Villeurbanne Cedex, France. [2]Unité de Génétique Moléculaire Murine, URA CNRS 1947, Institut Pasteur, 75015 Paris, France. [3]Genoscope, Centre National de Séquençage and CNRS UMR8030, Case Postale 5706, 91057 Evry Cedex, France.

*To whom correspondence should be addressed: E-mail: duret@biomserv.univ-lyon1.fr